On the Use of Hybrid CFIE-EFIE for Objects Containing Closed-Open Surface Junctions

Jinbo Liu, Jin Yuan, Wen Luo, Zengrui Li, *Member*, *IEEE*, and Jiming Song, *Fellow*, *IEEE*

***Abstract*—To effectively solve the electromagnetic scattering or radiation properties from the perfect electric conductor (PEC) objects containing closed-open surface junctions, how to establish the hybrid combined field integral equation-electric field integral equation (CFIE-EFIE) is studied, which is different with the existing scheme for the objects where the closed and open parts are separate. Further, it is found that when the integral equation is solved using the method of moments (MoM), if the widely used RWG basis functions are employed to expand the induced surface current, the CFIE-EFIE may give inaccurate numerical results for the objects containing fine structures. The numerical accuracy can be improved by introducing the linear-linear (LL) basis functions. Moreover, to pursue a high computational efficiency, the LL and RWG basis functions are simultaneously used to expand the current on the fine structures and other relatively smooth surfaces respectively, whose validity is verified by numerical results.**

***Index Terms*—Basis functions, iterative solution, method of moments, surface integral equations.**

I. Introduction

In the analysis of electromagnetic (EM) scattering or radiation properties, the integral equations in conjunction of the method of moments (MoM) are competitive approaches [1], [2]. During the numerical modeling of perfect electric conductor (PEC) objects which often contain both open and closed surfaces, traditionally, the electric field integral equation (EFIE) is formulated due to its independence of the surface type [3]. Unfortunately, for the closed PEC part, using the EFIE alone may encounter the interior resonance problem. Moreover, discretizing the EFIE which is a first-kind Fredholm integral equation usually yields an ill-conditioned matrix equation that is difficult to converge during the iterative solution. To avoid the interior resonance problem as well as to improve the matrix condition, some articles proposed the so-called hybrid combined field integral equation-electric field integral equation (CFIE-EFIE) [4]-[7]. That is, on the closed PEC parts of the objects establish the second-kind CFIE [8], which is derived from the linear combination of the EFIE and the magnetic field integral equation (MFIE), while the open parts still keep the EFIE. When the major part of the object is closed, the hybrid CFIE-EFIE can improve the solving efficiency substantially. Nevertheless, the existing articles only presented the discussions when the closed and open parts are separate [4]-[7], or dealt with the surface-wire junctions [9], [10]. For the objects containing closed-open surface junctions, the derivation of a rational CFIE-EFIE is more complicated, which will be shown in Section II of this letter.

In the process of MoM solution, the induced surface current is expanded with a series of basis functions. Because of the convenience of discretizing arbitrary surfaces and the quality of being free of pseudo line charges, the divergence-conforming RWG basis functions based on triangular patches are being widely used [3]. However, with the RWG basis functions, the numerical results from the MFIE are usually not as accurate as that from the EFIE [11]-[13]. This phenomenon will be more obvious when the calculated objects contain sharp edges or tips. Some researchers focused on looking for the reasons of this inaccuracy, such as the singularities arising in the outer integrals [11], [12], the improper expression of solid angle [13], and so on. Among them, the most likely one is that for the MFIE, the solution accuracy strongly depends on the quality of the current expression, while the "constant-normal" and "linear-tangential" RWG basis functions cannot properly represent an arbitrarily continuous current distribution [14], [15]. To overcome this problem, lots of novel basis functions were proposed [16]-[22]. The set of curl-conforming $\hat{n}\times$RWG basis functions was used to improve the MFIE accuracy, while it is not suitable for the solution of CFIE [16], [17]. The monopolar-RWG basis functions were proposed in [18] for the sharp-edged objects accurately solved by the MFIE, and were then combined with the RWG basis functions to form a hybrid discretization scheme for the CFIE implementation by setting the monopolar-RWG for those edges between non-coplanar triangles and the RWG for the others [19]. Besides, the linear-linear (LL) basis functions, also called as Trintinalia-Ling (TL) functions, which are "linear-normal" and "linear-tangential" and capable of expressing any linear current distribution, are attractive. The LL basis functions were first employed for the accurate solution of EFIE [20], and then extended to the MFIE and CFIE [21], [22]. It was shown that with the use of the LL functions, the results from the MFIE and CFIE can be significantly improved compared with the RWG functions.

This work was supported in part by the National Natural Science Foundation of China under Grant 61971384 and Grant 62071436, and in part by the Fundamental Research Funds for the Central Universities under Grant CUC210B013 and Grant CUC19ZD001. *(Corresponding authors: Jinbo Liu and Zengrui Li.)*

Jinbo Liu, Jin Yuan, Wen Luo, and Zengrui Li are with the State Key Laboratory of Media Convergence and Communication and the School of Information and Communication Engineering, Communication University of China, Beijing 100024, China (e-mail: liuj@cuc.edu.cn; zrli@cuc.edu.cn).

Jiming Song is with the Electrical and Computer Engineering, Iowa State University, Ames, Iowa 50011, USA (e-mail: jisong@iastate.edu).

However, since one LL basis function concurrently contains two linear vector functions associated with each common edge shared by two adjacent triangles, for a same object, the number of unknowns using the LL basis functions is the double of that using the RWG functions. As a result, the use of LL basis functions sacrifices the computational efficiency. As is well known, the distribution of induced current usually changes rapidly over the fine structures, while the change is slow for the smooth surfaces. Based on this fact, in this letter, the LL and RWG basis functions are simultaneously used to expand the surface current for the solution of the CFIE-EFIE, which will be established in Section II for the objects containing closed-open surface junctions. To be more specific, the LL basis functions are used to express the current on the fine structures, while the RWG basis functions are on other relatively smooth surfaces. The validity of this strategy is verified in Section III.

II. CFIE-EFIE Formulations and LL Basis Functions

Consider a PEC object in the free space that contains both closed surface S_c and open surface S_o, illuminated by an incident EM wave $\vec{E}^i$, $\vec{H}^i$ from an arbitrary direction. By vanishing the tangential component of total electric field, the EFIE is formed on all the open and closed surfaces [2], [3]. Imposing the boundary condition on the magnetic field over the closed surface S_c, the MFIE can be obtained and linearly added to the EFIE to form the so-called hybrid CFIE-EFIE as [4]-[6]

$$\text{CFIE} = \alpha(\vec{r})\,\text{EFIE} + \eta_0\beta(\vec{r})\,\text{MFIE} \tag{1}$$

where both α and β are $\vec{r}$ -dependent real combined coefficients, and η_0 is the intrinsic impedance of the free space. In [5], it was stated that $\beta(\vec{r}) = 1-\alpha(\vec{r})$, and $0<\alpha(\vec{r})<1$ when $\vec{r}\in S_c$ while $\alpha(\vec{r})=1$ for $\vec{r}\in S_o$. If the closed and open surfaces are totally separate, we can take the values of α and β like this without any doubt. On the contrary, however, if the object contains closed-open surface junctions where the closed and open surfaces have conjunct boundary, how to set up the values of α and β is worth further discussion.

Using the Galerkin's MoM, (1) is transformed into a generalized impedance matrix equation. During the current discretization, at the closed-open junctions, the basis functions are defined using the rule established in [23] to ensure no line charge accumulation. The matrix entry Z_{ji}, which denotes the interaction between the ith basis function $\vec{f}_i$ whose domain is S_i and the jth testing function $\vec{f}_j$ with domain S_j, is obtained by

$$\begin{aligned} Z_{ji} &= \mathrm{j}\omega\mu_0\int_{S_j}\alpha(\vec{r})\,\vec{f}_j(\vec{r})\bullet\int_{S_i}\vec{f}_i(\vec{r}')GdS'dS \\ &+\frac{\mathrm{j}}{\omega\varepsilon_0}\int_{S_j}\alpha(\vec{r})\,\vec{f}_j(\vec{r})\bullet\nabla\int_{S_i}\nabla'_S\bullet\vec{f}_i(\vec{r}')GdS'dS \\ &+\frac{\eta_0}{2}\int_{S_j}\beta(\vec{r})\,\vec{f}_j(\vec{r})\bullet\vec{f}_i(\vec{r})dS \\ &+\eta_0\int_{S_j}\beta(\vec{r})\,\vec{f}_j(\vec{r})\bullet\hat{n}(\vec{r})\times P.V.\int_{S_i}\vec{f}_i(\vec{r}')\times\nabla GdS'dS \end{aligned} \tag{2}$$

where $\mathrm{j}=\sqrt{-1}$, ε_0 and μ_0 are the permittivity and permeability of the free space, *P.V.* means the principal value integral, $\nabla'_S\bullet$ denotes the surface divergence operation, and $G=G(\vec{r},\vec{r}')$ is the Green's function in the free space. The jth element of the excitation vector is

$$V_j=\int_{S_j}\left[\alpha(\vec{r})\,\vec{f}_j(\vec{r})\bullet\vec{E}^i(\vec{r})+\eta_0\beta(\vec{r})\,\vec{f}_j(\vec{r})\bullet\hat{n}(\vec{r})\times\vec{H}^i(\vec{r})\right]dS \tag{3}$$

In (2), it is noticed that for the second term, the gradient operator is placed on the observation point $\vec{r}$, leading to a two -order singularity during $\vec{r}\to\vec{r}'$. To reduce the order of singularity, taking the surface Gauss theorem, the second term of (2) is usually transformed into

$$\begin{aligned} &\int_{S_j}\alpha(\vec{r})\,\vec{f}_j(\vec{r})\bullet\nabla\int_{S_i}\nabla'_S\bullet\vec{f}_i(\vec{r}')GdS'dS \\ &=\begin{Bmatrix}\int_{S_j}\nabla_S\bullet\left[\alpha(\vec{r})\,\vec{f}_j(\vec{r})\int_{S_i}\nabla'_S\bullet\vec{f}_i(\vec{r}')GdS'\right]dS \\ -\int_{S_j}\nabla_S\bullet\left[\alpha(\vec{r})\,\vec{f}_j(\vec{r})\right]\int_{S_i}\nabla'_S\bullet\vec{f}_i(\vec{r}')GdS'dS\end{Bmatrix} \\ &=\begin{Bmatrix}\int_{\partial S_j}\alpha(\vec{r})\left[\hat{n}_{\partial S_j}\bullet\vec{f}_j(\vec{r})\right]\int_{S_i}\nabla'_S\bullet\vec{f}_i(\vec{r}')GdS'dl \\ -\int_{S_j}\nabla_S\bullet\left[\alpha(\vec{r})\,\vec{f}_j(\vec{r})\right]\int_{S_i}\nabla'_S\bullet\vec{f}_i(\vec{r}')GdS'dS\end{Bmatrix} \end{aligned} \tag{4}$$

where $\hat{n}_{\partial S_j}$ denotes the outer-normal direction of ∂S_j, the boundary of S_j. Through this transformation, the singularity order is degraded to one. On the other hand, it is observed that the surface divergence operators are placed on not only the single $\vec{f}_i(\vec{r}')$ but also the product $\alpha(\vec{r})\,\vec{f}_j(\vec{r})$, both of which are then restricted to be divergence conforming. Under this restriction, if $\vec{r}\in S_j$ which belongs to a junctional region containing both the part of closed surface S_c and the part of open surface S_o, the value of $\alpha(\vec{r})$ for $\vec{r}\in S_c$ and that for $\vec{r}\in S_o$ must be the same. In other words, $\alpha(\vec{r})$ should be constant everywhere. Therefore, in the implementation, we set

$$\begin{aligned} &\alpha(\vec{r})=\alpha_0 \qquad\qquad \forall\vec{r}\in S_c+S_o \\ &\beta(\vec{r})=\begin{cases}1-\alpha(\vec{r}) & \forall\vec{r}\in S_c \\ 0 & \forall\vec{r}\in S_o\end{cases} \end{aligned} \tag{5}$$

while α_0 is constant and $0<\alpha_0<1$ (α_0 = 0.5 in all numerical examples presented later). Please note that mathematically, the values of α and β in (2) depend on the position of observation point, but not the row number of the matrix equation as [4]-[6].

In the choice of basis functions to solve the CFIE-EFIE, because there is no accumulation of pseudo line charges, the divergence-conforming RWG basis functions are widely used [3]. However, as mentioned above, the set of RWG basis functions cannot express arbitrary current distribution, while the MFIE is sensitive to the accuracy of current expression. Therefore, if the CFIE-EFIE that contains MFIE is used to model the object, the use of RWG basis functions may lead to inaccurate results. To express the surface current more accurately, a set of LL basis functions has been developed [20]-[22]. Similar to the RWG basis functions, the LL basis functions are also defined on pairs of adjacent triangles. The LL basis function shares the following two properties with the RWG basis function: 1) Its normal component on the common edge is continuous when across the common edge, while that on the non-common edges is strictly equal to zero. 2) Its surface divergence is piecewise uniform which is inversely proportional to the corresponding triangle area, accomplishing charge neutrality over the pair of adjacent triangular patches. Actually, adding the two linear functions of the ith LL function can obtain the ith RWG function. Due to this property, the

computational code using the LL basis functions can be obtained by modifying the conventional one using the RWG basis functions easily, while the LL and RWG basis functions can be simultaneously used to discretize objects without worrying about the mesh boundary continuity.

III. Numerical Validations

In the following calculations, the GMRES with a restart number 100 is used as the iterative solver to reach 0.001 residual error [24]. All calculations are executed serially on a workstation with 3.2 GHz CPU and 16 GB RAM.

In the first case, using the RWG basis functions, the bistatic radar cross section (RCS) at *xoz* plane of a PEC semisphere of radius 1.5λ clung to a square plate of side length 3.1λ, propagating along the negative z-axis, is calculated. After discretization with an average 0.1λ mesh size, the numbers of triangles on the closed semisphere part and the other open part are 5,304 and 576, respectively, which results in 8,805 unknowns. The numerical results from the EFIE and CFIE-EFIE (CFIE for the closed semisphere and EFIE for the remaining open part) are shown in Fig. 1. In addition, the CFIE-EFIE result from the wrong choice of $\alpha(\vec{r})$, i.e., $\alpha(\vec{r})$ is 0.5 for $\vec{r} \in S_c$ and 1 for $\vec{r} \in S_o$, is also given. It is observed that the results from the EFIE and CFIE-EFIE are almost in excellent agreement everywhere, while the result with wrong α shows a totally unacceptable difference. It states that for simple objects, the rational use of the CFIE-EFIE companied with the RWG basis functions can give reliable results. During the iterative solution, the CFIE-EFIE reaches the convergence with 81 iterations and 1.6 s CPU time, about four times faster than the EFIE converged after 329 iterations with 6.1 s CPU time. On the other hand, if the area of the bottom plate becomes larger, the advantage of the CFIE-EFIE on the convergence speed will be weaker. That is to say, the CFIE-EFIE is actually effective only when the closed part occupies a main proportion of the calculated object.

In the second case, the radiation patterns and the input impedances of a monopole mounted on the center of a PEC box are calculated at 300 MHz. The size of the box is 1 m × 1 m × 0.1 m, and the length and width of the strip-shaped monopole are 0.25 m and 0.01 m, respectively. After discretizing, the number of triangles is 546. In the CFIE-EFIE implementation, the EFIE and CFIE are applied to the open PEC monopole and the six faces of the closed PEC box, respectively. The monopole is fed with a delta-function voltage source associated with the common edge that belongs to the closed-open surface junction. According to [25, (4.2)], the incident electric field within the edge can be expressed as $\vec{E}^i = -\nabla\varphi$ with the electric potential φ. From the Maxwell's equation $\nabla \times \vec{E}^i = -\mathrm{j}\omega\mu_0\vec{H}^i$, we have $\vec{H}^i \equiv 0$. Therefore, when the integral in (3) is executed over the closed triangular patches that contains the feed edge, the second term of the kernel related to the magnetic field is zero. The calculated radiation patterns are shown in Fig. 2, while the input impedances as well as the computational details such as the numbers of unknowns and iterations are listed in Table I. For comparison, the result from the EM simulation software Altair FEKO [26] is also shown as the baseline. It is observed that compared with the FEKO result, the EFIE one shows a good agreement, while the CFIE-EFIE result has a clear difference. The maximum difference of the radiation patterns between the FEKO and CFIE-EFIE results occurring over the peak range (2.62 dBi vs. 1.62 dBi at about 56 °) is about 1 dB. Physically, besides the monopole part, the top face of the box also has a big influence on the numerical results, while the influence of other five faces is believed to be slight. Modeled by the CFIE-EFIE and expanded by the RWG basis functions, the normalized magnitude of the current density on the top face of the PEC box is shown in Fig. 3 (a). It is evident that the center current nearby the fine feed port mightily changes and abruptly varies on both sides of the common edge. As the CFIE-EFIE solution accuracy involving the MFIE strongly depends on the quality of current expression, the result difference in Fig. 2 between RWG&EFIE and RWG&CFIE-EFIE implementations is obvious.

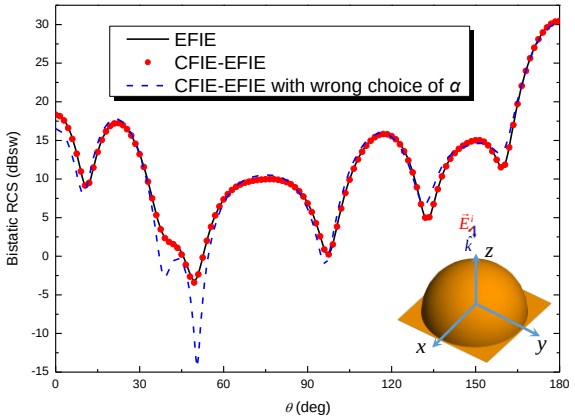

Fig. 1. Bistatic RCS of a PEC semisphere of radius 1.5λ clung to a square plate of side length 3.1λ.

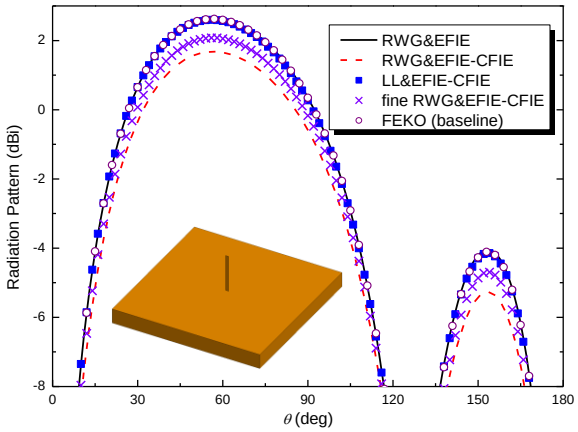

Fig. 2. Radiation patterns of a 0.25m×0.01m strip-shaped monopole mounted on a 1m×1m×0.1m PEC box at 300 MHz using different implementations.

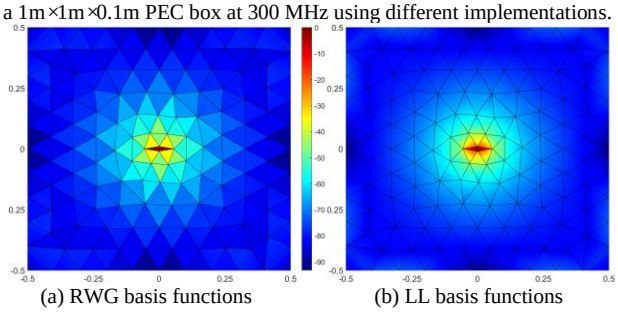

(a) RWG basis functions (b) LL basis functions

Fig. 3. Normalized magnitude (in dB) of the current density solved by the CFIE-EFIE on the top face of the PEC cube, on whose center the striped monopole is mounted.

This article has been accepted for publication in a future issue of this journal, but has not been fully edited. Content may change prior to final publication. Citation information: DOI 10.1109/LAWP.2021.3077143, IEEE Antennas and Wireless Propagation Letters

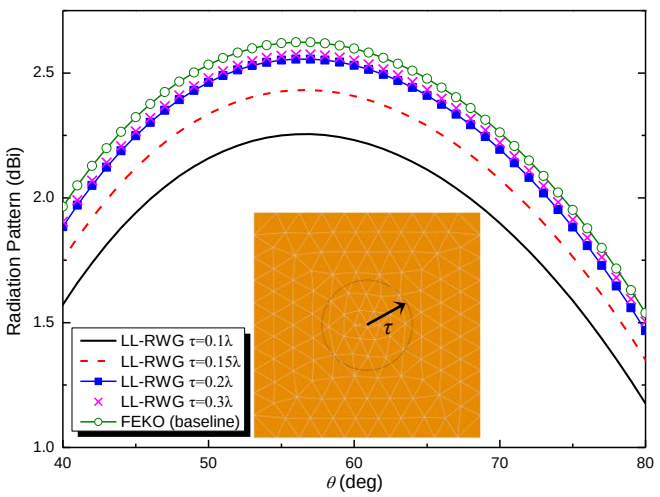

Fig. 4. Radiation patterns nearby the peak range using LL-RWG strategy with different values of τ to determine the LL region.

TABLE I
COMPUTATIONAL DETAILS FOR DIFFERENT IMPLEMENTATIONS, INPUT IMPEDANCE FROM FEKO IS 42.8+J27.0

Strategy	UN	IE	IN	Time (s)	MD (dB)	Input impedance
RWG	814	EFIE	93	2.31	0.02	42.9+j26.9
		CE	28	0.84	1.01	57.7+j18.6
LL	1,628	CE	57	3.92	0.03	43.6+j25.7
fine RWG	3,208	CE	121	10.1	0.54	51.9+j23.1
LR τ=0.1λ	832	CE	30	0.87	0.37	46.4+j24.6
LR τ=0.15λ	848		32	0.90	0.19	45.0+j25.2
LR τ=0.2λ	874		35	1.02	0.06	44.1+j25.4
LR τ=0.3λ	922		49	1.49	0.05	43.9+j25.5

Note - CE: CFIE-EFIE, LR: LL-RWG, UN: unknowns number, IE: integral equation, IN: iterations number, Time: total CPU time, MD: maximal difference over the peak range between the computational and the FEKO results.

To express the surface current more accurately, using the LL basis functions, the monopole object is recalculated, while the numerical results and computational details are also shown in Fig. 2 and Table I, respectively. For comparison, we remesh the whole object with a fine mesh size and use the RWG basis functions alone to expand the current (denoted by fine RWG). It is seen that when the LL basis functions are used, the result from the CFIE-EFIE is in quite agreement with the FEKO result, which demonstrates that the accuracy problem of the CFIE-EFIE arising from the RWG basis functions can be mitigated by employing the LL basis functions. The normalized magnitude of the current density on the top face is shown in Fig. 3 (b). As expected, the current behavior obtained from the LL basis functions is clearly smoother than that from the RWG basis functions, which illustrates that the LL basis functions provide a much better representation of the current distribution. This is also the main reason why the result accuracy from the CFIE-EFIE can be improved. On the other hand, the fine meshes with the RWG basis functions have a very limited role in improving the numerical accuracy. In other words, when the RWG basis functions are used, the numerical accuracy cannot be significantly improved just through a fine-mesh scheme.

However, the cost of the improvement using the LL is that the number of unknowns is doubled, resulting in more memory usage, relatively slow convergence during the iterative solution, and long total CPU time, as shown in Table I. To alleviate this problem, the necessity of the LL basis functions is analyzed carefully. Logically, because of the location of the fine feed port, the magnitude of the current density on the center of the top face of the PEC cube is distinctly larger than other regions and drastically changes, where the discontinuity of the current distribution is then obvious. The phenomenon shown in Fig. 3 conforms to this anticipation. Due to this fact, we discretize the closed box parts modeled by the CFIE using different kinds of basis functions simultaneously, i.e., the LL basis functions are used to express the center region of the top face which contains the fine feed port, while the RWG basis functions are to other parts (denoted by LL-RWG). Since the striped monopole is modeled by the EFIE, it is still expressed by the RWG basis functions. On the choice of the LL and the RWG regions, we use a flexible mesh information-based strategy with the following filtering criterion

$$\begin{cases} \left|\vec{r}_m^{\,c} - \vec{r}_{\text{feed}}^{\,c}\right| \le \tau & T_m \in \text{LL region} \\ \text{otherwise} & T_m \in \text{RWG region} \end{cases} \tag{6}$$

where $\vec{r}_m^{\,c}$ and $\vec{r}_{\text{feed}}^{\,c}$ are the centers of the triangle T_m on the top face and the feed port, respectively, and τ is a tuning parameter. In the LL-RWG strategy, the computational accuracy and efficiency can be conveniently controlled by setting different τ. Please note that for this monopole object, the distance between some triangles on the bottom face and the feed port center may be also smaller than τ, but because the bottom face is not illuminated by the monopole directly, these triangles also belong to the RWG region. Under this criterion, with different values of τ, the numerical results and computational details are shown in Fig. 4 and Table I, respectively. It is found that the LL-RWG strategy does an excellent job on improving the calculation accuracy with slightly more unknowns and an acceptable convergence rate. When τ=0.2λ, the maximal difference over the peak range between the result from FEKO and that from the CFIE-EFIE with the LL-RWG (2.62 dBi vs. 2.56 dBi) is about 0.06 dB. Through massive numerical experiments, it is found that τ=0.2λ can give an acceptable accuracy for most radiation problems.

IV. CONCLUSION

In this letter, the hybrid CFIE-EFIE is presented to model the objects that contain closed-open surface junctions. In the MoM solution, when the RWG basis functions are used to expand the current distribution, because the RWG basis functions cannot properly expand the current distribution, the CFIE-EFIE may result in less accurate solutions. The LL basis functions are introduced to solve this problem. Nevertheless, the number of unknowns using the LL basis functions is twice of that using the RWG basis functions, leading to a better accuracy but less efficient. To break this limitation, we use the RWG and LL basis functions to discretize different parts of the objects simultaneously according to their structural characters, while a criterion with a tuning parameter to determine how to choose the LL region is proposed. Numerical results show that this strategy has an acceptable accuracy with a high efficiency.

REFERENCES

[1] R. F. Harrington, *Field Computation by Moment Methods*. MacMillan, New York, 1968.

[2] W. C. Chew, J. M. Jin, E. Michielssen, and J. M. Song, *Fast and Efficient Algorithms in Computational Electromagnetics*, Boston, MA, USA: Artech House, 2001.

[3] S. M. Rao, D. R. Wilton, and A. W. Glisson, "Electromagnetic scattering by surfaces of arbitrary shape," *IEEE Trans. Antennas Propag.*, vol. 30, no. 3, pp. 409–418, May 1982.

[4] L. Gürel and Ö. Ergül, "Extending the applicability of the combined-field integral equation to geometries containing open surfaces," *IEEE Antennas Wireless Propag. Lett.*, vol. 5, pp. 515-516, 2006.

[5] Ö. Ergül and L. Gürel, "Iterative solutions of hybrid integral equations for coexisting open and closed surfaces," *IEEE Trans. Antennas Propag.*, vol. 57, no. 6, pp. 1751-1758, Jun. 2009.

[6] Z. H. Fan, D. Z. Ding, and R. S. Chen, "The efficient analysis of electromagnetic scattering from composite structures using hybrid CFIE-IEFIE," *Progress In Electromagnetics Research B*, vol. 10, pp. 131-143, 2008.

[7] B. Karaosmanoğlu, C. Önol, and Ö. Ergül, "Optimizations of EFIE and MFIE combinations in hybrid formulations of conducting bodies," in *2015 International Conference on Electromagnetics in Advanced Applications (ICEAA)*, Turin, Italy, Oct. 2015, pp. 1276-1279.

[8] P. Ylä-Oijala and M. Taskinen, "Calculation of CFIE impedance matrix elements with RWG and $n\times$RWG functions," *IEEE Trans. Antennas Propag.*, vol. 51, no. 8, pp. 1837-1846, Aug. 2003.

[9] H. Y. Chao, J. S. Zhao, and W. C. Chew, "Application of curvilinear basis functions and MLFMA for radiation and scattering problems involving curved pec structures," *IEEE Trans. Antennas Propag.*, vol. 51, no. 2, pp. 331-336, Feb. 2003.

[10] W. B. Ewe, L. W. Li, C. S. Chang, and J. P. Xu, "AIM analysis of scattering and radiation by arbitrary surface-wire configurations," *IEEE Trans. Antennas Propag.*, vol. 55, no. 1, pp. 162-166, Jan. 2007.

[11] Ö. Ergül and L. Gürel, "Investigation of the inaccuracy of the MFIE discretized with the RWG basis functions," *in Proc. 2004 IEEE AP-S Int. Symp.*, Monterey, CA, USA, Dec. 2004, vol.3, pp.3393-3396.

[12] L. Gürel and Ö. Ergül, "Singularity of the magnetic-field integral equation and its extraction," *IEEE Antennas Wireless Propag. Lett.*, vol. 4, pp. 229-232, 2005.

[13] J. M. Rius, E. Úbeda, and J. Parrón, "On the testing of the magnetic field integral equation with RWG basis functions in method of moments," *IEEE Trans. Antennas Propag.*, vol. 49, no. 11, pp. 1866-1868, Dec. 2001.

[14] R. D. Graglia, D. R. Wilton, and A. F. Peterson, "Higher order interpolatory vector bases for computational electromagnetics," *IEEE Trans. Antennas Propag.*, vol. 45, no. 3, pp. 329-342, Mar. 1997.

[15] J. Wang and J. P. Webb, "Hierarchal vector boundary elements and p-adaption for 3-D electromagnetic scattering," *IEEE Trans. Antennas Propag.*, vol. 45, no. 12, pp. 1869-1879, Dec. 1997.

[16] E. Ubeda and J. M. Rius, "MFIE MoM-formulation with curl-conforming basis functions and accurate kernel integration in the analysis of perfectly conducting sharp-edged objects," *Microw. Opt. Techn.Lett.*, vol. 44, no. 4, pp. 354–358, 2005.

[17] Ö. Ergül and L. Gürel, "The use of curl-conforming basis functions for the magnetic-field integral equation," *IEEE Trans. Antennas Propag.*, vol. 54, no. 7, pp. 1917-1926, Jul. 2006.

[18] E. Ubeda and J. M. Rius, "Novel monopolar MFIE MoM-discretization for the scattering analysis of small objects," *IEEE Trans. Antennas Propag.*, vol. 54, no. 1, pp. 50-57, Jan. 2006.

[19] E. Ubeda, I. Sekulic, J. M. Rius, and A. Heldring, "Accurate, grid-robust and versatile combined- field discretization for the electromagneticscattering analysis of perfectly conducting targets," *J. Comput. Physics*, vol. 407, p. 109236, Apr. 2020.

[20] L. C. Trintinalia and H. Ling, "First order triangular patch basis functions for electromagnetic scattering analysis," *J. of Electromagn. Waves and Appl.*, vol. 15, no. 11, pp. 1521-1537, 2001.

[21] Ö. Ergül and L. Gürel, "Improving the accuracy of the magnetic field integral equation with the linear-linear basis functions," *Radio Sci.*, vol. 41, no. 4, pp. 1-15, Aug. 2006.

[22] Ö. Ergül and L. Gürel, "Linear-linear basis functions for MLFMA solutions of magnetic-field and combined-field integral equations," *IEEE Trans. Antennas Propag.*, vol. 55, no. 4, pp. 1103-1110, Apr. 2007.

[23] B. M. Kolundzija, "Electromagnetic modeling of composite metallic and dielectric structures," *IEEE Trans. Microw. Theory Tech.*, vol. 47, no. 7, pp. 1021-1032, Jul. 1999.

[24] Y. Saad and M. H. Schultz, "GMRES: A generalized minimal residual algorithm for solving nonsymmetric linear systems," *SIAM J. Sci. and Stat. Comput.*, vol. 7, no. 3, pp. 856-869, 1986.

[25] S. N. Makarov, "Dipole and monopole antennas: the radiation algorithm," in *Antenna and EM Modeling with MATLAB*, Houston, USA: Princeton University Press, 2002, ch. 4, pp. 57-88.

[26] Altair. (2014). *FEKO, Suite 7.0* [Online]. Available: https://www.altair.com/feko